Unit-sphere description of nematic flows

Tomas Carlsson
Institute of Theoretical Physics, Chalmers University of Technology, S-412 96 Göteborg, Sweden
(Received 15 January 1985; revised manuscript received 5 March 1986)

The unit-sphere description of nematic liquid-crystal configurations first introduced by Thurston [J. Appl. Phys. 52, 3040 (1981)] and dealing with elastic properties of nematic liquid crystals only is extended to include also the study of nematic flows. It is shown how the general features of the flow properties of nematic liquid crystals can be studied by the mapping of the hydrodynamic torque on the unit sphere. The effects of the application of electric or magnetic fields to a nematic liquid crystal under shear are discussed by adding the corresponding torque to the maps. Introducing a dimensionless quantity ε, which is the ratio of the hydrodynamic and the electric (magnetic) torques, one can deduce whether the hydrodynamic effects are dominating over the field effects or vice versa. By drawing the sequence of torque maps which appears as ε goes from minus to plus infinity [ε having the same sign as the dielectric (magnetic) anisotropy] it is shown how one can get a good qualitative understanding of the flow behavior just by the inspection of these maps. By calculating the eigenvalues of the singular points of the torque maps, their stability is determined. The stable ones correspond to flow alignment of the director, while the unstable ones can lend themselves to the study of hydrodynamic instabilities. It is also shown how one in a simple manner can derive expressions of relaxation times, boundary layers, and thresholds of hydrodynamic instabilities by knowing the eigenvalues of the singular points. Finally, it is proven that the equations governing the director profile are formally equivalent to those of a particle moving on a smooth sphere upon which the hydrodynamic torque pattern is imposed, the elastic constant (in the one-constant approximation) playing the same role as the mass of the particle. Using this equivalence it is discussed how one can approach the shear-flow problem of nematic liquid crystals by using the powerful tools of analytical mechanics.

I. INTRODUCTION

The flow behavior of nematic liquid crystals is a subject which lends itself to the study of many fascinating and unexpected phenomena. Starting with the works of Anzelius[1] and Oseen,[2] the theoretical basis for the understanding of the viscoelastic properties of nematic liquid crystals was finally formulated by Leslie[3] and Ericksen[4] who showed that a complete description of the problem needs six viscosity coefficients. By the Parodi relation[5] these six are reduced into five linearly independent viscosities. Using the convention adopted by Leslie we denote the viscosity coefficients by α_i $(i=1-6)$. When studying the qualitative flow behavior of nematic liquid crystals there are, however, only two of these that are of importance: α_2 and α_3. These must fulfill[3] one important restriction,

$$\gamma_1 \equiv \alpha_3 - \alpha_2 > 0 \ . \tag{1.1}$$

Due to this inequality the signs of α_2 and α_3 can combine in three different ways: (a) $\alpha_2 < \alpha_3 < 0$; (b) $\alpha_3 > 0$, $\alpha_2 < 0$; (c) $\alpha_3 > \alpha_2 > 0$. While case (a) leads to the well-known situation of flow alignment,[6] case (b) turns out to exhibit different kinds of instabilities which have been studied both experimentally[7-12] and theoretically.[13-15] The possibility that compounds with viscosity coefficients belonging to case (c) could be found among the disklike nematic liquid crystals has on theoretical grounds been proposed by Carlsson.[16,17]

In this paper we study the shear flow of nematic liquid crystals under the following restrictions. We confine the nematic between two parallel glass plates, one at rest while the other one is moved with the velocity v_0. Neglecting transverse flow effects[18] and also keeping v_0 below the critical value where roll instabilities[19] occur, the aim is to calculate the director and the velocity profile through the sample.

II. VISCOELASITIC EQUATIONS: CHOICE OF COORDINATE SYSTEM

The problem which we study is pictured in Fig. 1. We confine the liquid crystal between two parallel glass plates, distance d apart, the lower one at rest while the upper one is moving with the velocity v_0. The z axis is taken perpendicular to the plates and the director is given by the unit vector $\hat{\mathbf{n}}$. Assuming strong anchoring conditions at the boundaries, the goal is to calculate the velocity profile $v(z)$ (neglecting transverse flow effects the velocity is given by $\mathbf{v}=v\hat{\mathbf{x}}$) and the director profile $\hat{\mathbf{n}}(z)$. Each direction of the director generates a point on the unit sphere and the director profile $\hat{\mathbf{n}}(z)$ is thus given by a path (parametrized by z) on the unit sphere connecting the two points given by the boundary conditions. By introducing spherical polar coordinates each point on the unit sphere is assigned to the angles θ and φ. This unit-sphere description was first introduced by Thurston[20] who studied pure elastic problems, but here we will extend it to the

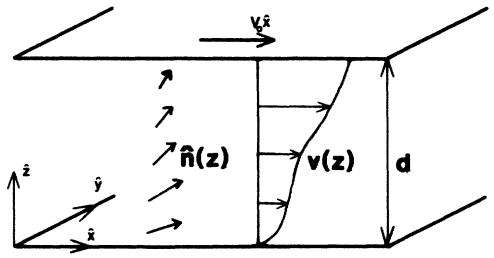

FIG. 1. Geometry of the shear-flow problem. The liquid crystal is confined between two glass plates, distance d apart, both parallel to the xy plane. The lower one is at rest while the upper one is moving in the x direction with the velocity v_0. The aim is to calculate the director and the velocity profile $\hat{\mathbf{n}}(z)$ and $v(z)$, respectively. These are determined—at every specified set of external conditions—by five viscosity coefficients and three elastic constants.

case of nematic flows.

In order to avoid that the solution path passes close to the pole of the coordinate system we introduce two different ways of introducing this according to Fig. 2. We either orient the pole along the z direction (coordinate system I) or along the y direction (coordinate system II). All quantities which belong to system I will be labeled with a subscript 1, while all quantities corresponding to system II will be labeled with a subscript 2.

The next task is to formulate the viscoelastic equations using the two different coordinate systems introduced above. A general coordinate-invariant way of formulating these equations is given by Leslie.[3,21] Applying Leslie's equations to our special choices of coordinates now gives two sets of equations, one for system I and one for system II. We end up with three coupled differential equations in each case:[22] two for the director profile determining $\theta(z)$ and $\varphi(z)$ and one for the velocity profile determining $v(z)$,

$$\tfrac{1}{2}(\theta')^2F_{,\theta}+\tfrac{1}{2}(\varphi')^2(2G_{,\varphi}-H_{,\theta})+\theta'\varphi'F_{,\varphi}+\theta''F+\varphi''G+\Gamma^s_{\varphi}+\Gamma^r_{\varphi}=0\ , \quad (2.1)$$

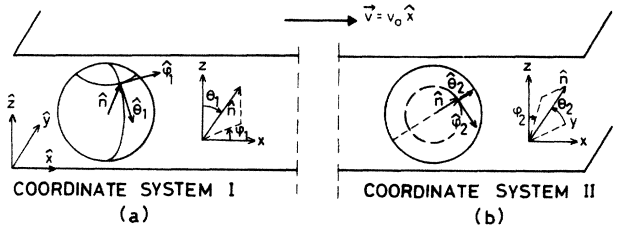

FIG. 2. Coordinate systems used in this work are conventional spherical polar ones. Coordinate system I (a) has the pole oriented in the z direction, while in the case of coordinate system II (b) the pole is in the y direction. In this way we can always find a proper coordinate system, in which the director paths do not pass close to a coordinate singularity, for any problem which we want to study.

$$\tfrac{1}{2}(\theta')^2(2G_{,\theta}-F_{,\varphi})+\tfrac{1}{2}(\varphi')^2H_{,\varphi}+\theta'\varphi'H_{,\theta}+\theta''G+\varphi''H-\sin\theta(\Gamma^s_{\theta}+\Gamma^r_{\theta})=0\ , \quad (2.2)$$

$$u'=\frac{dv}{dz}=\frac{\tau}{g(\theta,\varphi)}+\frac{f(\theta,\varphi)\dot{\theta}+h(\theta,\varphi)\dot{\varphi}}{g(\theta,\varphi)}\ . \quad (2.3)$$

In writing Eqs. (2.1)–(2.3) we have used the shorthand notation $\theta'=(d\theta/dz)$; $\varphi'=(d\varphi/dz)$; $G_{,\varphi}=(dG/d\varphi)$, etc. We have also introduced τ which is the shearing force per unit area. K_1, K_2, and K_3 are the Frank elastic constants and α_i $(i=1-6)$ are the Leslie viscosities. The auxiliary functions F, G, and H, the viscous torques Γ^s_{θ}, Γ^s_{φ}, Γ^r_{θ}, and Γ^r_{φ}, and the viscous functions g, f, and h read in the two-coordinate systems. System I is as follows:

$$\begin{aligned}
&F_1=K_1\sin^2\theta_1+K_3\cos^2\theta_1\ ,\\
&G_1=0\ ,\\
&H_1=K_2\sin^4\theta_1+K_3\sin^2\theta_1\cos^2\theta_1\ ,
\end{aligned} \quad (2.4)$$

$$\begin{aligned}
&\Gamma^s_{\theta_1}=-u'\alpha_2\cos\theta_1\sin\varphi_1\ ,\\
&\Gamma^s_{\varphi_1}=u'(\alpha_3\sin^2\theta_1-\alpha_2\cos^2\theta_1)\cos\varphi_1\ ,
\end{aligned} \quad (2.5)$$

$$\begin{aligned}
&\Gamma^r_{\theta_1}=\gamma_1\sin\theta_1\dot{\varphi}_1\ ,\\
&\Gamma^r_{\varphi_1}=-\gamma_1\dot{\theta}_1\ ,
\end{aligned} \quad (2.6)$$

$$\begin{aligned}
g_1(\theta_1,\varphi_1)&=\tfrac{1}{4}\alpha_1\sin^2(2\theta_1)\cos^2\varphi_1+\tfrac{1}{2}(\alpha_6-2\alpha_2-\alpha_3)\cos^2\theta_1\\
&\quad+\tfrac{1}{2}(\alpha_3+\alpha_6)\sin^2\theta_1\cos^2\varphi_1+\tfrac{1}{2}\alpha_4\ ,\\
f_1(\theta_1,\varphi_1)&=\cos\varphi_1(\alpha_3\sin^2\theta_1-\alpha_2\cos^2\theta_1)\ ,\\
h_1(\theta_1,\varphi_1)&=\alpha_2\cos\theta_1\sin\theta_1\sin\varphi_1\ .
\end{aligned} \quad (2.7)$$

System II is as follows:

$$\begin{aligned}
&F_2=K_1\cos^2\theta_2\cos^2\varphi_2+K_2\sin^2\varphi_2+K_3\sin^2\theta_2\cos^2\varphi_2\ ,\\
&G_2=(K_2-K_1)\sin\theta_2\cos\theta_2\sin\varphi_2\cos\varphi_2\ ,\\
&H_2=K_1\sin^2\theta_2\sin^2\varphi_2+K_2\sin^2\theta_2\cos^2\theta_2\cos^2\varphi_2+K_3\sin^4\theta_2\cos^2\varphi_2\ ,
\end{aligned} \quad (2.8)$$

$$\begin{aligned}
&\Gamma^s_{\theta_2}=u'\sin\theta_2(\alpha_2\cos^2\varphi_2-\alpha_3\sin^2\varphi_2)\ ,\\
&\Gamma^s_{\varphi_2}=-(\alpha_2+\alpha_3)u'\sin\theta_2\cos\theta_2\sin\varphi_2\cos\varphi_2\ ,
\end{aligned} \quad (2.9)$$

$$\begin{aligned}
&\Gamma^r_{\theta_2}=\gamma_1\sin\theta_2\dot{\varphi}_2\ ,\\
&\Gamma^r_{\varphi_2}=-\gamma_1\dot{\theta}_2\ ,
\end{aligned} \quad (2.10)$$

$$\begin{aligned}
g_2(\theta_2,\varphi_2)&=\tfrac{1}{4}\alpha_1\sin^4\theta_2\sin^2(2\varphi_2)+\tfrac{1}{2}(\alpha_6-2\alpha_2-\alpha_3)\sin^2\theta_2\cos^2\varphi_2\\
&\quad+\tfrac{1}{2}(\alpha_3+\alpha_6)\sin^2\theta_2\sin^2\varphi_2+\tfrac{1}{2}\alpha_4\ ,\\
f_2(\theta_2,\varphi_2)&=-(\alpha_2+\alpha_3)\sin\theta_2\cos\theta_2\sin\varphi_2\cos\varphi_2\ ,\\
h_2(\theta_2,\varphi_2)&=\sin^2\theta_2(\alpha_3\sin^2\varphi_2-\alpha_2\cos^2\varphi_2)\ .
\end{aligned} \quad (2.11)$$

To summarize, the governing equations of the shear-flow problem are Eqs. (2.1)—(2.3). For the different choices of coordinate systems given by Fig. 2 we substitute either Eqs. (2.4)—(2.7) or Eqs. (2.8)—(2.11) into these.

While all the physics of the system is given by the previous equations, in practice, these coupled differential equations are hard to solve except in some special cases. Furthermore, even if one succeeds in finding a solution path to a particular problem, the question of its stability against nearby lying paths is an even harder problem. We will show in Sec. III that by the mapping of the shearing torque Γ^s on the unit sphere, one gains a fairly good qualitative understanding of the general features of the system. In the subsequent sections we then show that by this mapping we can solve the problem of the bulk motion (i.e., neglecting elasticity) exactly. Furthermore, we show that by introducing elasticity in the one-constant approximation, we can reformulate the problem into another more familiar one, which makes it more transparent than just writing down a set of differential equations.

III. MAPPING OF THE SHEARING TORQUE ON THE UNIT SPHERE

The viscous torque Γ^v which is acted upon the director can be divided into two parts: the shearing torque $\Gamma^s=\Gamma^s_{\theta}\hat{\theta}+\Gamma^s_{\varphi}\hat{\varphi}$, which is due to the shearing of the medium and the rotational torque, $\Gamma^r=\Gamma^r_{\theta}\hat{\theta}+\Gamma^r_{\varphi}\hat{\varphi}$, which will act upon the director in a nonstationary state. The consequence of the shearing torque Γ^s acting on the director in a state given by a point (θ,φ) on the unit sphere will be to rotate the director with the momentary axis of rotation given by Γ^s. As is shown in Fig. 3, θ and φ will then change according to

$$\Delta\theta\sim\Gamma^s_{\varphi},\quad \Delta\varphi=-\frac{\Gamma^s_{\theta}}{\sin\theta}\ . \tag{3.1}$$

The minus sign in the last of Eqs. (3.1) comes from the fact that a rotation along the positive $\hat{\theta}$ axis corresponds to decreasing φ and the factor $\sin\theta$ is due to that when

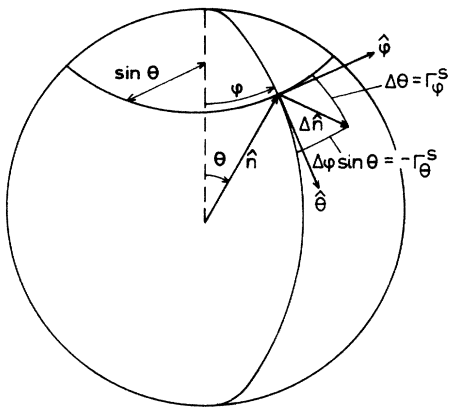

FIG. 3. The effect of the shearing torque $\Gamma^s=\Gamma^s_{\theta}\hat{\theta}+\Gamma^s_{\varphi}\hat{\varphi}$ is to rotate the director with the momentary axis of rotation given by Γ^s. The change of the director is then given by $\Delta\hat{\mathbf{n}}\sim(\Gamma^s_{\varphi}\hat{\theta}-\Gamma^s_{\theta}/\sin\theta\hat{\varphi})$.

changing φ, the director travels along a circle on the unit sphere, which has a radius of $\sin\theta$. At any point on the unit sphere we have now singled out a direction given by Eqs. (3.1) telling us which way the director will rotate under the influence of the shear. Dividing these equations with each other we instead get an equation defining the path which will be traced out by the director under the influence of the shear (neglecting elasticity). This is given by

$$\frac{d\varphi}{d\theta}=-\frac{\Gamma^s_{\theta}}{\Gamma^s_{\varphi}\sin\theta}\ . \tag{3.2}$$

By plotting the torque maps on the unit sphere we directly get a feeling of what is going on as we shear a nematic. In Fig. 4 we have displayed a sequence of torque maps for the different combinations of the signs of α_2 and α_3 which are possible, and also for different values of the crucial parameter α_3/α_2. We have drawn the plots as polar plots, using the coordinates of system II, where the equator ($\theta_2=\pi/2$; $\varphi_2\varepsilon[0,2\pi]$) represents the shearing plane. Due to the symmetry of the director ($\hat{\mathbf{n}}$ and $-\hat{\mathbf{n}}$ are equivalent) we only have to study half of the unit sphere. The arrows on the paths indicate which way the director will rotate under the action of the shear. The singular points of the torque field are the possible equilibrium orientations of the director. The stable equilibrium points are either a stable node (SN) or a center (C), and the unstable ones are either an unstable node (UN) or a saddle point (SP).

Studying the case when both α_2 and α_3 are negative, we immediately recognize the features of the flow. Starting at any point on the sphere, the director will end up at the point given by $\theta_2=\pi/2$; $\tan\varphi_2=(\alpha_2/\alpha_3)^{1/2}$ or on its physically equivalent antipole. This is the well-known flow alignment angle. We also find two unstable equilibrium points. These may be realized at low shear rates, when the elastic torque from the boundaries can compensate the destabilizing torque which will act on the director in the vicinity of these points. One of these [$\theta_2=\pi/2$; $\tan\theta_2=-(\alpha_2/\alpha_3)^{1/2}$] is an unstable node, while the other one ($\theta_2=\varphi_2=0$) is a saddle and represents the geometry of the homogeneous instability which is discussed by Pieranski and Guyon.[23] This instability has also been examined theoretically by Maneville and Dubois-Violette[24] who have calculated its threshold using a method different but equivalent to the one presented in Sec. VI C of this paper.

Focusing our attention on the case when α_3 is positive, α_2 still being negative, we find only one (stable) equilibrium point at $\theta_2=\varphi_2=0$. This is a center. One interesting question concerning this case is what happens when we shear the liquid crystal, starting with the director in the shearing plane. In the bulk case (neglecting elasticity) we see that a fluctuation that brings the director out of the shearing plane will not tend to bring it further away. The director will just trace out a path, which closely follows the original one. However, Pieranski *et al.*[9] have reported this flow to be unstable against fluctuations which tend to bring the director out of the plane of shear if the shear rate exceeds a critical value. In order to understand this problem thoroughly we have to include elasticity and we postpone the discussion of this instability until Sec. VIII.

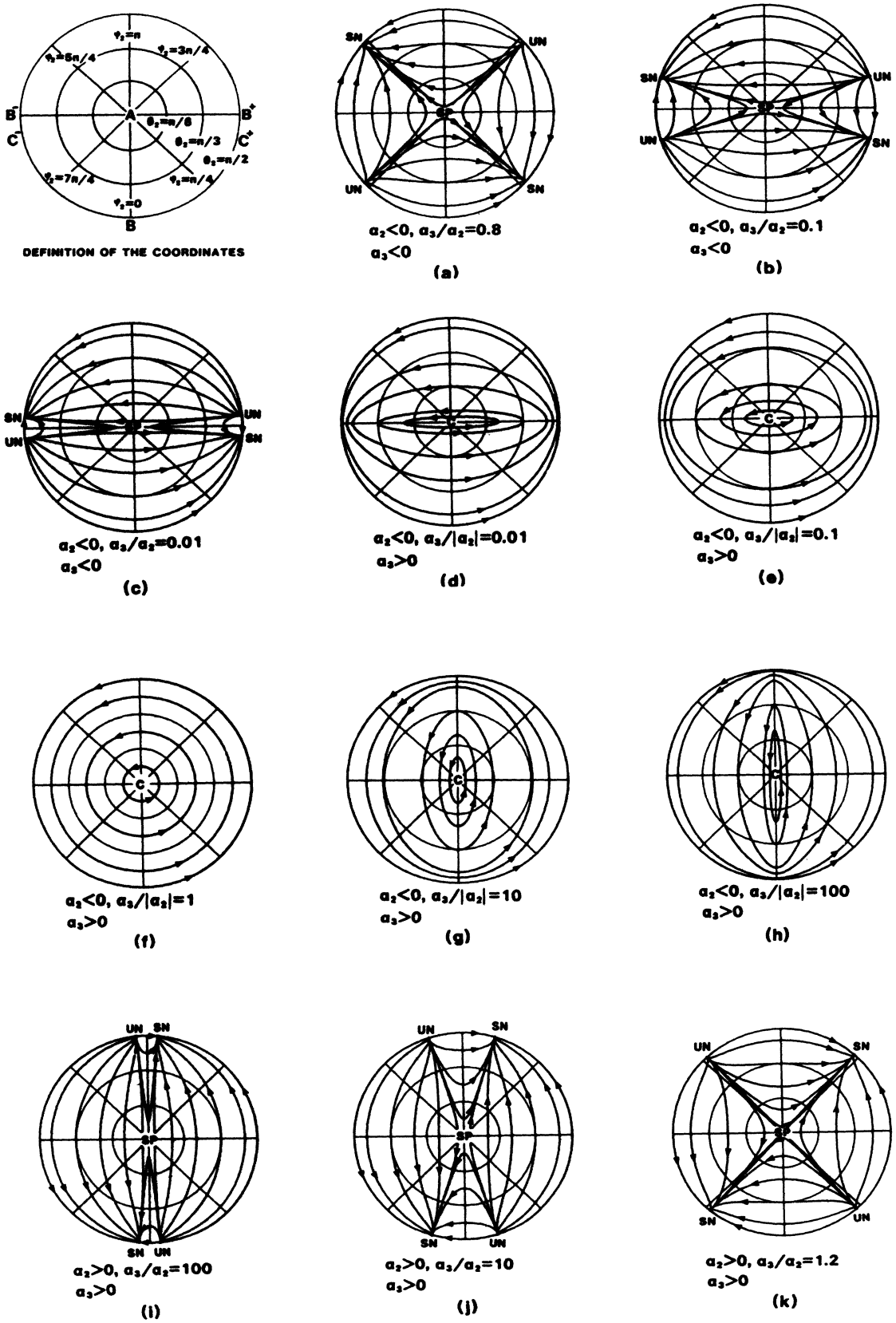

FIG. 4. Torque maps of nematic flows. We can distinguish three topologically distinct cases: (1) $\alpha_2<\alpha_3<0$, (a)—(c); (2) $\alpha_2<0$, $\alpha_3>0$, (d)—(h); (3) $\alpha_3>\alpha_2>0$, (i)—(k).

Finally, if we study the case when both α_2 and α_3 are positive, we see that the torque maps resemble the case when they are both negative with some important exceptions. First of all the arrows of the torque maps are reversed implying that the stable equilibrium is now given by $\theta_2=\pi/2$; $\tan\varphi_2=-(\alpha_2/\alpha_3)^{1/2}$ while the point $\theta_2=\pi/2$; $\tan\varphi_2=(\alpha_2/\alpha_3)^{1/2}$ now gets unstable. Also the inequality (1.1) demands that $\alpha_3>\alpha_2$. This has the consequence that the equilibrium points now fall into the interval $\theta_2=\pi/2$; $\varphi_2\varepsilon[-\pi/4,\pi/4]$ in contrast to what is the case when both α_2 and α_3 are negative. The possibility that nematic liquid crystals consisting of disklike molecules belong to the case of positive α_2 and α_3 have been suggested by Carlsson.[16,17]

IV. MAPPING OF THE TORQUE FROM ELECTRIC AND MAGNETIC FIELDS ON THE UNIT SPHERE

In this section we study the effects of applying electric or magnetic fields to a nematic. Using SI units the corresponding torque can be written[25]

$$\mathbf{\Gamma}^{\varepsilon}=\delta\hat{\mathbf{n}}\cdot\hat{\mathbf{B}}(\hat{\mathbf{n}}\times\hat{\mathbf{B}})\ , \tag{4.1}$$

where $\hat{\mathbf{B}}$ is a unit vector in the direction of the field and δ is a coupling constant which is given by

$$\begin{aligned}&\delta=\frac{\chi_a}{\mu_0}B^2\ \text{(magnetic case)}\ ,\\ &\delta=\epsilon_a\epsilon_0E^2\ \text{(electric case)}\ .\end{aligned} \tag{4.2}$$

In Eqs. (4.2) we have introduced the vacuum permeability μ_0, the magnetic anisotropy χ_a, the dielectric anisotropy ϵ_a, the applied magnetic induction $\mathbf{B}$, and the applied electric field $\mathbf{E}$. We notice the formal equivalence between the torques which appear in the electric and the magnetic cases. Many effects which are studied by the application of an electric field can be reproduced by the use of a magnetic field—it is just the coupling constant δ which differs. However, while in the magnetic case the magnetic induction is constant throughout the sample (if homogeneous from the beginning) irrespective of the variation of the director in space, in the electric case a spatial varying director will cause the electric field to be inhomogeneous. Thus, we have to interpret the torque maps in the electric case with some caution.

We now apply a field $\mathbf{B}$ to the nematic. The director is specified by a polar coordinate system. In this system the direction of the field is given by the polar angles $\tilde{\theta}$ and $\tilde{\varphi}$. The field torque is then given by[22]

$$\begin{aligned}\Gamma^{\varepsilon}_{\theta}=&\delta[\sin\theta\sin^2\tilde{\theta}\sin(\varphi-\tilde{\varphi})\cos(\varphi-\tilde{\varphi})\\ &+\cos\theta\sin\tilde{\theta}\cos\tilde{\theta}\sin(\varphi-\tilde{\varphi})]\ ,\\ \Gamma^{\varepsilon}_{\varphi}=&\tfrac{1}{2}\delta[\cos(2\theta)\sin(2\tilde{\theta})\cos(\varphi-\tilde{\varphi})-\sin(2\theta)\cos^2\tilde{\theta}\\ &+\sin(2\theta)\sin^2\tilde{\theta}\cos^2(\varphi-\tilde{\varphi})]\ .\end{aligned} \tag{4.3}$$

The consequence of this torque is to force the director to point in a direction parallel ($\delta>0$) or perpendicular ($\delta<0$) to $\mathbf{B}$, respectively.

V. BULK MOTION: COMBINATION OF HYDRODYNAMIC AND FIELD TORQUE MAPS

We are now in a position to discuss the bulk motion of the system. Neglecting elasticity in Sec. III, we saw that the director just traces out the torque path on the unit sphere defined by its initial position. The trace point of the director behaves like a massless particle moving on a smooth sphere upon which we have imposed a force field given by the torque maps drawn in Figs. 4–6. The particle is viscously damped according to $\mathbf{F}^{\text{visc}}=-\gamma_1\mathbf{v}$, where $\mathbf{v}$ is the velocity of the particle.

Studying a flow with a magnetic field applied we have to construct torque maps according to Eq. (3.2) using the combined torque $\mathbf{\Gamma}=\mathbf{\Gamma}^{s}+\mathbf{\Gamma}^{\varepsilon}$. First we have to determine the singular points of these torque maps, examine their stability, and classify them. Neglecting elasticity, Eqs. (2.1) and (2.2) can, by the use of Eqs. (2.6) or (2.10), be transformed into

$$\begin{aligned}&\gamma_1\dot{\theta}=\Gamma^{s}_{\varphi}+\Gamma^{\varepsilon}_{\varphi}\ ,\\ &\gamma_1\dot{\varphi}=-\frac{1}{\sin\theta}(\Gamma^{s}_{\theta}+\Gamma^{\varepsilon}_{\theta})\ .\end{aligned} \tag{5.1}$$

The nature of an equilibrium point (θ^0,φ^0) is now determined by the eigenvalues λ_1 and λ_2 of the matrix a_{ij} which defines the linearized version of Eqs. (5.1) in the vicinity of the corresponding point.[26] In this way we now investigate some cases and show how one can get useful information of the qualitative flow behavior just by the plotting of the corresponding torque maps. Apart from what is discussed in Sec. III we will also find stable (SF) and unstable (UF) foci among the singular points of the torque maps.

All torque maps will be displayed using coordinate system II, which is better adopted to the symmetry of the problem than system I. All plots will be drawn as polar plots according to the upper left part of the figures. The angle which the director makes with the y axis, θ_2, increases radially outwards from the center of the plot, which is denoted by A. The equator $\theta_2=\pi/2$; $\varphi_2\varepsilon[0,2\pi]$ represents the shearing plane. The point B ($\theta_2=\pi/2$; $\varphi_2=0$) represents the situation when the director is perpendicular to the glass plates. The points B^+ and B^- both represent the situation when the director is parallel to the glass plates, still being within the plane of shear. The points C^+ and C^- on the equator are the points where the angle between the director and the normal to the plates is arctan $(|\alpha_2/\alpha_3|)^{1/2}$. As we will frequently find the pole of system II to be an equilibrium point, we use system I in the mathematical treatment of the problem.

It might be helpful to get a rough estimate of when the field torque dominates over the shearing torque and vice versa. Defining ε as

$$\varepsilon=\frac{\delta}{\delta_c}=\frac{\delta}{2u'(|\alpha_2\alpha_3|)^{1/2}} \tag{5.2}$$

we shall find $|\varepsilon|$ as a convenient dimensionless quantity of measuring the field strength. ε can be positive or negative depending on the sign of the magnetic (dielectric) anisotropy of the nematic. When $|\varepsilon|\gg1$ field effects

dominate the behavior of the flow while the hydrodynamic effects are dominating when $|\varepsilon| \ll 1$.

We first investigate the case when $\alpha_2<0$, $\alpha_3>0$, and the applied field is in the z direction. Equations (2.5), (4.3), and (5.1) then give

$$\gamma_1\dot{\theta}_1=u'(\alpha_3\sin^2\theta_1-\alpha_2\cos^2\theta_1)\cos\varphi_1-\tfrac{1}{2}\delta\sin(2\theta_1)\,,$$
$$\gamma_1\dot{\varphi}_1=u'a_2\cot\theta_1\sin\varphi_1\,. \tag{5.3}$$

In this case the point A ($\theta_1^0=\varphi_1^0=\pi/2$) is an equilibrium point. The linearized version of Eqs. (5.3) in this case reads

$$\gamma_1\dot{\alpha}=\delta\alpha-u'\alpha_3\beta,\quad \gamma_1\dot{\beta}=-u'\alpha_2\alpha\,, \tag{5.4}$$

where α and β are the deviations of θ and φ from their equilibrium positions, respectively. The eigenvalues of a_{ij} are given by

$$\lambda_{1,2}=u'(|\alpha_2|\alpha_3)^{1/2}[\varepsilon\pm(\varepsilon^2-1)^{1/2}]\,. \tag{5.5}$$

If $|\varepsilon|<1$ (weak fields) the eigenvalues are complex. The equilibrium is thus a stable or an unstable focus depending on the sign of ε. In the limiting case of zero field it becomes a center. If $|\varepsilon|>1$ (strong fields) the eigenvalues are real and distinct, both having the same sign as ε. The equilibrium then is a stable ($\varepsilon<-1$) or an unstable ($\varepsilon>1$) node.

We will also, for strong enough fields, find two equilibrium points on the equator. These can be written

$$\tan\theta_1^0=\left[\frac{|\alpha_2|}{\alpha_3}\right]^{1/2}[\varepsilon\pm(\varepsilon^2-1)^{1/2}],\quad \varphi_1^0=0\quad(\varepsilon>0)$$
$$\tan\theta_1^0=\left[\frac{|\alpha_2|}{\alpha_3}\right]^{1/2}[|\varepsilon|\pm(\varepsilon^2-1)^{1/2}],\quad \varphi_1^0=\pi\quad(\varepsilon<0)\,. \tag{5.6}$$

If $|\varepsilon|>1$ the solution of Eqs. (5.6) are real and in this case the linearized version of Eqs. (5.3) in the vicinity of the singular points are

$$\gamma_1\dot{\alpha}=2u'[(\alpha_2+\alpha_3)\sin\theta_1^0\cos\theta_1^0 -\varepsilon(|\alpha_2|\alpha_3)^{1/2}\cos(2\theta_1^0)]\alpha\,,$$
$$\gamma_1\dot{\beta}=u'\alpha_2\cot\theta_1^0\beta\quad(\varepsilon>1)$$
$$\gamma_1\dot{\alpha}=-2u'[(\alpha_2+\alpha_3)\sin\theta_1^0\cos\theta_1^0 +\varepsilon(|\alpha_2|\alpha_3)^{1/2}\cos(2\theta_1^0)]\alpha\,, \tag{5.7}$$
$$\gamma_1\dot{\beta}=-u'\alpha_2\cot\theta_1^0\beta\quad(\varepsilon<-1)\,.$$

The corresponding eigenvalues can be written

$$\lambda_1=\pm 2u'(|\alpha_2|\alpha_3)^{1/2}(\varepsilon^2-1)^{1/2}\,,$$
$$\lambda_2=u'\alpha_2\cot\theta_1^0<0\quad(\varepsilon>1)\,;$$
$$\lambda_1=\mp 2u'(|\alpha_2|\alpha_3)^{1/2}(\varepsilon^2-1)^{1/2}\,, \tag{5.8}$$
$$\lambda_2=-u'\alpha_2\cot\theta_1^0>0\quad(\varepsilon<-1)\,;$$

where the upper sign in Eqs. (5.8) corresponds to the upper one in Eqs. (5.6). In the case of positive ε we thus will find one saddle and one stable node, while we in the case of negative ε will find one saddle and one unstable node. We then get the following sequence of equilibrium points as ε goes from minus to plus infinity (in Fig. 5 the corresponding torque maps are drawn in the case $\alpha_3=10|\alpha_2|$).

(1) $\varepsilon<-1$. The point A is a stable node while there are one saddle and one unstable node located at the equator between B^- and B, the saddle lying between B^- and C^- and the unstable node between C^- and B. When $\varepsilon\to-1$ the saddle and the unstable node coalesce at C^-.

(2) $-1<\varepsilon<0$. When $\varepsilon=-1$ the stable node at A transforms into a stable focus being the only equilibrium point in this case. The equator is now an unstable limit cycle.

(3) $\varepsilon=0$. This is the limiting case between positive and negative anisotropy which occurs when the field is zero. The point A is now a center.

(4) $0<\varepsilon<1$. The point A is now an unstable focus while the equator becomes a stable limit cycle.

(5) $\varepsilon>1$. In this case A is an unstable node while there are one stable node and one saddle located on the equator between B and B^+. When $\varepsilon=1$ these bifurcate at C^+, the stable node moving towards B as the field increases while the saddle is moving towards B^+.

The second case we investigate is the one when both α_2 and α_3 are negative while the field is applied in the y direction. Equations (2.5), (4.3), and (5.1) then give

$$\gamma_1\dot{\theta}_1=u'(\alpha_3\sin^2\theta_1-\alpha_2\cos^2\theta_1)\cos\varphi_1 +\tfrac{1}{2}\delta\sin(2\theta_1)\sin^2\varphi_1\,,$$
$$\gamma_1\dot{\varphi}_1=u'\alpha_2\cot\theta_1\sin\varphi_1+\tfrac{1}{2}\delta\sin(2\varphi_1)\,. \tag{5.9}$$

Analyzing these equations in the same manner as Eqs. (5.3) will give the following sequence of equilibrium points as ε goes from minus to plus infinity (in Fig. 6 the corresponding torque maps are drawn in the case $\alpha_2=10\alpha_3$).

(1) $\varepsilon<-\frac{1}{2}$. The point A is an unstable node while there are one stable node and one saddle located in the shearing plane at the points C^+ [$\tan\theta_1^0=(\alpha_2/\alpha_3)^{1/2}$; $\varepsilon_1^0=0$] and C^- [$\tan\theta_1^0=(\alpha_2/\alpha_3)^{1/2}$, $\varphi_1^0=\pi$] respectively.

(2) $\varepsilon=-\frac{1}{2}$. There still is a stable node located at C^+ but the whole meridian through A and C^- now represent unstable equilibrium positions.

(3) $-\frac{1}{2}<\varepsilon<\frac{1}{2}$. When $\varepsilon=-\frac{1}{2}$ the saddle and the unstable node change places so now there is a saddle at A, an unstable node at C^-, and a stable node at C^+.

(4) $\varepsilon=\frac{1}{2}$. The unstable node at C^- remains but the whole meridian through A and C^+ now represents stable equilibrium positions.

(5) $\varepsilon>\frac{1}{2}$. When $\varepsilon=\frac{1}{2}$ the saddle and the stable node change places so now there is a stable node at A, a saddle at C^+, and an unstable node at C^-.

A more complete survey of the torque maps and the eigenvalues of the corresponding singular points for all possible combinations of α_2 and α_3 (the field being in the x, y, or z direction) is given elsewhere.[22]

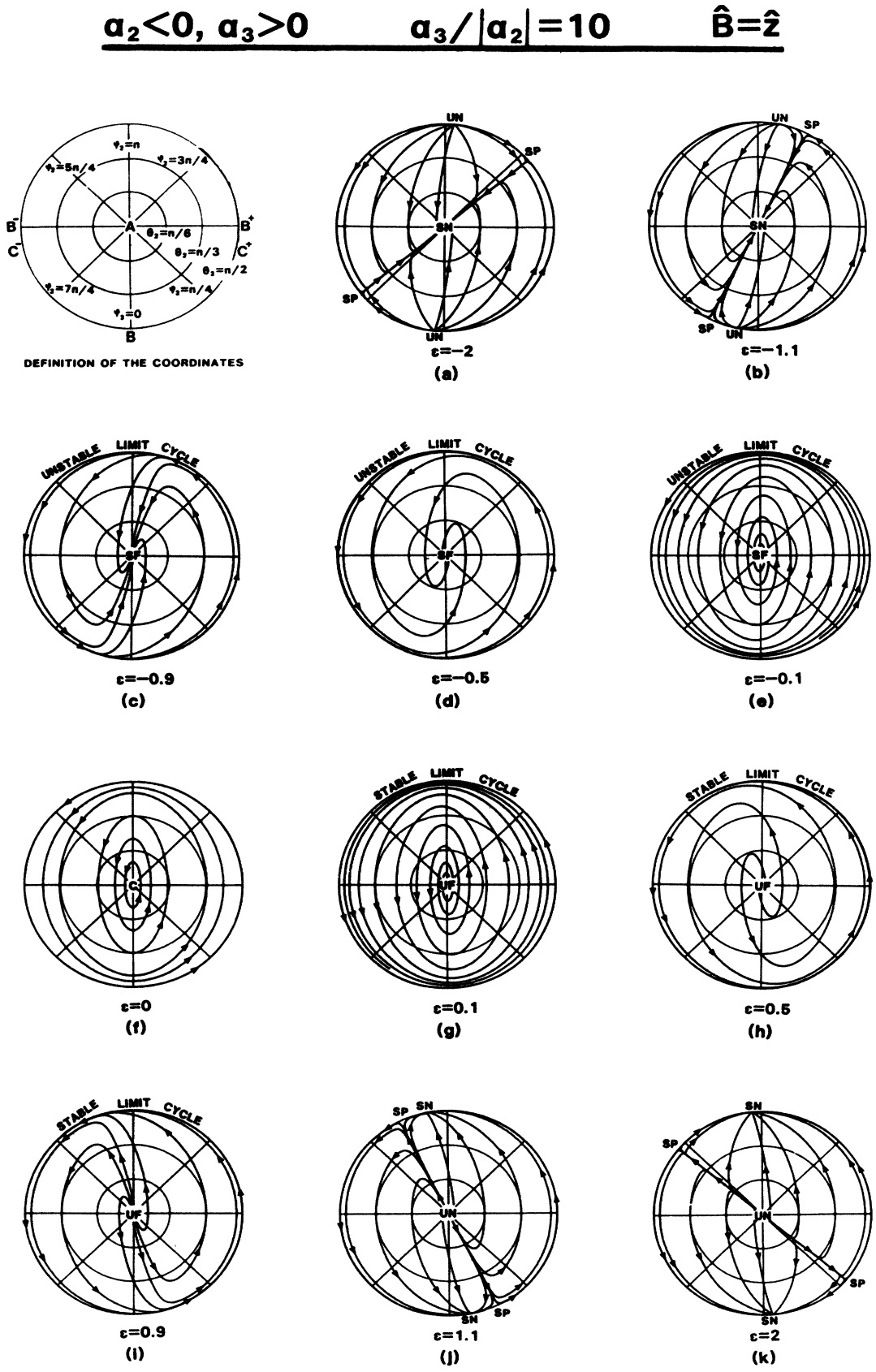

FIG. 5. Torque maps of the nematic flow in the case $\alpha_2<0$, $\alpha_3>0$, the applied field being in the z direction. We distinguish five topologically distinct cases depending on the value of the field strength ε: (1) $\varepsilon<-1$, (a)—(b); (2) $-1<\varepsilon<0$, (c)—(e); (3) $\varepsilon=0$, (f); (4) $0<\varepsilon<1$, (g)—(i); (5) $\varepsilon>1$, (j)—(k).

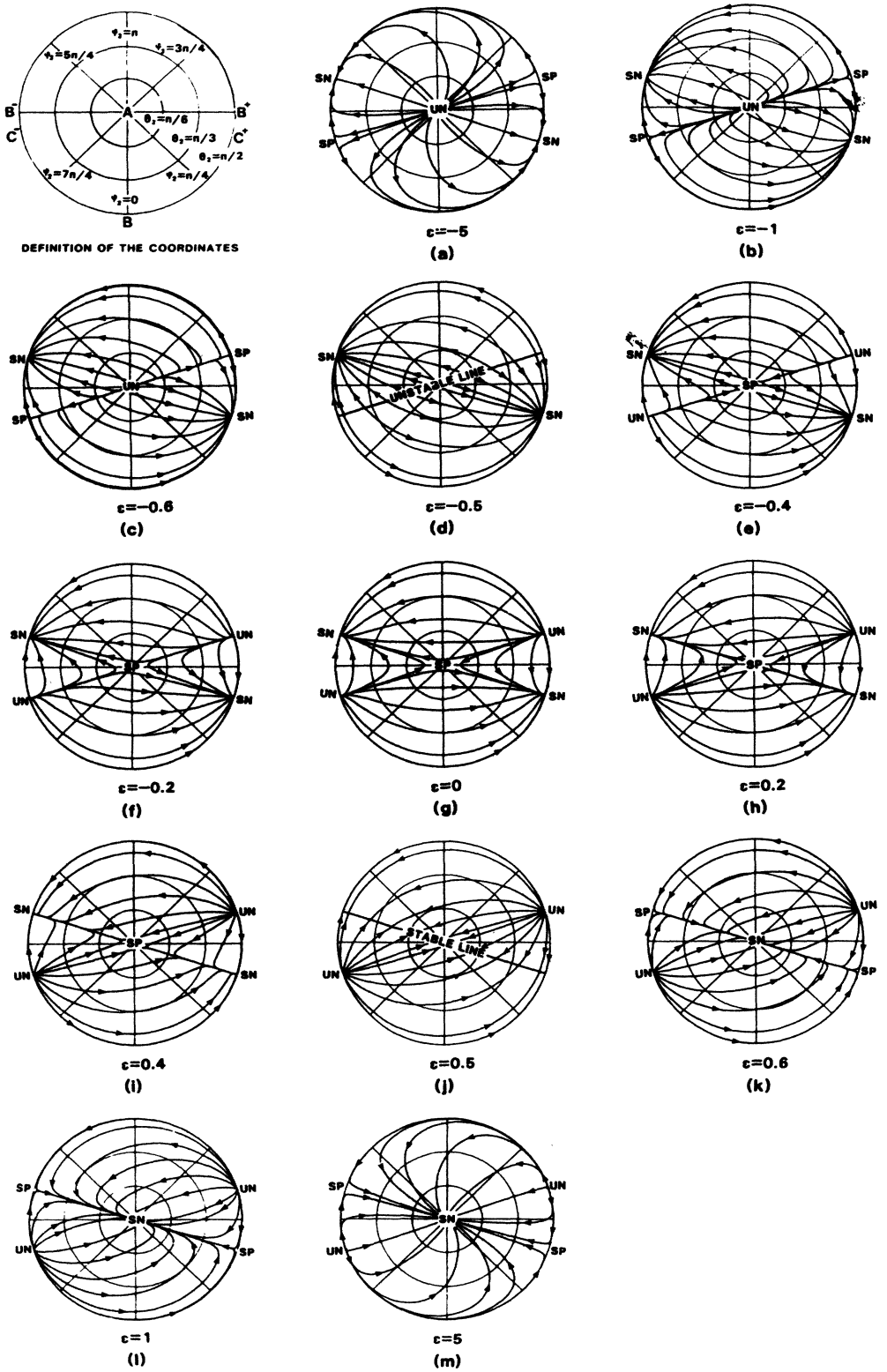

FIG. 6. Torque maps of the nematic flow in the case $\alpha_2 < 0$, $\alpha_3 < 0$, the applied field being in the y direction. We distinguish five topologically distinct cases depending on the value of the field strength ε: (1) $\varepsilon < -0.5$, (a)—(c); (2) $\varepsilon = -0.5$, (d); (3) $|\varepsilon| < 0.5$, (e)—(i); (4) $\varepsilon = 0.5$, (j); (5) $\varepsilon > 0.5$, (k)—(m).

VI. MEANING OF THE EIGENVALUES: RELAXATION TIMES, BOUNDARY LAYERS AND INSTABILITIES

In Sec. V we were motivated to calculate the eigenvalues of the linearized version of the torque equations (5.1) in order to determine the nature of the equilibrium points of the torque maps. Below we will show how these eigenvalues can be used to make estimations of relaxation times, boundary layers, and thresholds of hydrodynamic instabilities.

A. Relaxation times

We start this section by posing the question: If the director starts in the vicinity of a stable equilibrium point, what will be the time scale for its relaxation back to this equilibrium? This question is—neglecting elasticity—answered by examining the linearized version of Eqs. (5.1). Introducing new coordinates α^1 and β^1, in which the matrix a_{ij} is diagonalized, it is easy to convince oneself that a disturbance (θ_0^1,φ_0^1) will die out in an exponential way characterized by two relaxation times τ_1 and τ_2. If the equilibrium is a stable node, the eigenvalues of a_{ij}, λ_1 and λ_2 are both negative, and τ_1 and τ_2 are given by

$$\tau_1=\frac{\gamma_1}{|\lambda_1|},\quad \tau_2=\frac{\gamma_1}{|\lambda_2|}\ . \tag{6.1}$$

If, on the other hand, the equilibrium is a stable focus, the eigenvalues are complex conjugates having a negative real part $\lambda_{1,2}=\lambda_0\pm i\kappa$. The relaxation time is still controlled by the real part of λ ($\lambda_0<0$). In this case, however, the director will spiral towards the equilibrium point with an angular velocity $\omega=\kappa/\gamma_1$.

B. Boundary layers

If the director in some way is forced to point in a direction other than its equilibrium one, we will be interested in calculating the penetration depth ξ of this disturbance. The disturbance may be due to an impurity in the liquid crystal, a disclination, or preferably to the boundary conditions imposed by the treatment of the glass plates, in which case it will give rise to a boundary layer type of flow.

We want to study the time-independent solution of Eqs. (2.1) and (2.2) in the vicinity of a stable equilibrium point. For simplicity we perform the analysis within the one-constant approximation $K_1=K_2=K_3=K$. By again introducing a coordinate system with its origin in the equilibrium point in question and rotating it in a proper way we can write the linearized version of Eqs. (2.1) and (2.2) as

$$K\frac{d^2\alpha^1}{dz^2}+\lambda_1\alpha^1=0,\quad K\frac{d^2\beta^1}{dz^2}+\lambda_2\beta^1=0\ , \tag{6.2}$$

where λ_1 and λ_2 still are the eigenvalues of the matrix a_{ij}. As the equilibrium is assumed to be a stable one the real parts of λ_1 and λ_2 are negative. Equations (6.2) thus represent an exponential decay towards the equilibrium characterized by the two penetration depths ξ_1 and ξ_2,

$$\xi_1=(K/|\lambda_{1r}|)^{1/2},\quad \xi_2=(K/|\lambda_{2r}|)^{1/2}\ , \tag{6.3}$$

where λ_{1r} and λ_{2r} are the real parts of λ_1 and λ_2, respectively.

C. Instabilities

In Secs. VI A and VI B we discussed the properties of the flow in the vicinity of the stable equilibrium points. We now go on by investigating the unstable equilibrium points, which may lend themselves to the study of hydrodynamic instabilities in the following manner: We prepare the glass plates in such a way that the boundary conditions coincide with the director orientation of one of the unstable equilibrium points. At a low shearing rate the director profile will still be constant throughout all the sample because a director fluctuation which normally would bring the director away from its initial position will be stabilized by the elasticity. At a critical shearing rate u_c', however, the elasticity no longer can master the situation and the director moves away seeking up one of its stable equilibrium positions. In a recent work Högfors and Carlsson[15] study the stability of the in-plane flow of nematic liquid crystals i.e., a flow of the type $\theta_2=\pi/2$, $\varphi_2=\varphi_2(z)$. The instabilities which are studied in this paper are of a much simpler nature than those studied by Högfors and Carlsson, because now we start with a director configuration which is constant in space $\theta_2(z)=\theta_2^0$, $\varphi_2(z)=\varphi_2^0$. Using the results of Högfors and Carlsson we can formulate the stability criterion as

$$\lambda_1<K\frac{\pi^2}{d^2},\quad \lambda_2<K\frac{\pi^2}{d^2}\ , \tag{6.4}$$

where λ_1 and λ_2 are the real parts of the eigenvalues connected with the equilibrium point, d is the thickness of the sample, and K is the elastic constant. For the instability to occur only one of the inequalities (6.4) has to be violated and consequently it is the largest of the eigenvalues which determine the threshold of the instability. We thus can gain insight in which direction the instability will set in by comparing the magnitudes of the eigenvalues. Here, however, caution must be made for uncritical use of (6.4) because the one-constant approximation in many cases is a crude one, so in order to make a definite statement concerning this question we have to rederive the inequalities (6.4) in the case of unequal elastic constants.

VII. ROLE OF THE ELASTICITY

In Secs. III and V we showed how we could get a good qualitative understanding of the flow properties of nematic liquid crystals just by the inspection of the torque maps. In Sec. VI we pushed the analysis further by introducing elasticity and restricting the flow to be only in the vicinity of the equilibrium points. The general question—the calculation of the time-independent director profile and the determination of its stability in the case of arbitrary boundary conditions—has, however, not been discussed, and below we show how one can deal with this problem within the unit-sphere approach.

The expression of the elastic energy density can, within the one-constant approximation, be written[20]

$$w=\tfrac{1}{2}K\left[\frac{d^2\theta}{dz^2}+\sin^2\theta\frac{d^2\varphi}{dz^2}\right], \tag{7.1}$$

an expression valid for both the coordinate systems introduced in Sec. II. Because of this we do not label θ and φ by any indices throughout this section. By introducing the arc length S on the unit sphere we can, by the use of the relation $dS^2=d\theta^2+\sin^2\theta\, d\varphi^2$, write the elastic energy density as

$$w=\tfrac{1}{2}K\left[\frac{dS}{dz}\right]^2. \tag{7.2}$$

The pure elastic problem (i.e., without flow and/or field effects) is now solved by minimizing the total free energy W of the sample. The trajectory traced out by the director is thus the one which minimizes the integral

$$W=\int_{z_0}^{z_1}\tfrac{1}{2}K\left[\frac{dS}{dz}\right]^2 dz\ . \tag{7.3}$$

We now for a moment turn to an entirely different problem, namely, that of a particle of mass m which is moving on a smooth sphere. The solution of this problem can be formulated by Hamilton's principle as:[27] "The particle will trace out the trajectory on the sphere for which the action integral I is stationary." If no forces act upon the particle the action integral is

$$I=\int_{t_0}^{t_1}\tfrac{1}{2}m\left[\frac{dS}{dt}\right]^2 dt\ , \tag{7.4}$$

where $\frac{1}{2}m\,(dS/dt)^2$ is the kinetic energy of the particle. We thus notice the formal equivalence between the elastic problem of nematic liquid crystals and the problem of a free particle moving on a smooth sphere. The elastic constant in the first case plays the same role as the mass in the second one. Furthermore, in the elastic problem the solution path is parametrized by the space coordinate z, while it is time which parametrizes the solution path in the particle case.

We now want to extend the analysis from the pure elastic case to the one where we introduce flow as well as the influence of applied electric or magnetic fields. The effect of this extension is to impose a "force field" upon the unit sphere. This force field is, of course, the field which is visualized in the torque maps of Figs. 4–6. The solution path of the time-independent shear-flow problem will thus be the same as that of a particle moving on a smooth sphere upon which we have imposed the same field. We now show how this analogy can be derived from basic principles in a more formal way. The governing equations of the director profile in the stationary case are given by Eqs. (2.1) and (2.2). These read putting $K_1=K_2=K_3=K$,

$$\begin{aligned} &K\left[\frac{d^2\theta}{dz^2}-\sin\theta\cos\theta\left[\frac{d\varphi}{dz}\right]^2\right]+\Gamma_\varphi=0\ ,\\ &K\left[\sin\theta\frac{d^2\varphi}{dz^2}+2\cos\theta\frac{d\theta}{dz}\frac{d\varphi}{dz}\right]-\Gamma_\theta=0\ . \end{aligned} \tag{7.5}$$

The Γ's in Eqs. (7.5) are now considered to be the sum of the shearing torque and the field torque, i.e., $\Gamma_i=\Gamma_i^s+\Gamma_i^e$. Making the substitution $K\to -m$, $z\to t$, $\Gamma_\varphi\to F_\theta$, and $\Gamma_\theta\to -F_\varphi$, these equations transform to those of a particle moving on a smooth sphere under the influence of the force field $\mathbf{F}=F_\theta\hat{\theta}+F_\varphi\hat{\varphi}$. The conclusion drawn is the following: *The stationary shear-flow problem of nematic liquid crystals is equivalent to the study of the motion of a particle of negative mass moving on a smooth sphere upon which we have imposed a force field* $(\Gamma_\varphi,-\Gamma_\theta)$. *The elastic constant K plays the role of the negative mass $-m$ of the particle. The z coordinate parametrizes the trajectory, playing the role of time in the particle motion.* One could ask oneself whether it would not be better to let the elastic constant play the role of a positive mass, instead of defining the force field with the opposite sign than what is done. This would indeed give the same torque maps apart from the arrows being turned into the opposite direction. Therefore we would be misled concerning the stability of the singular points, because those with the arrows going inwards really are the stable equilibrium points of the torque maps.

The conclusion which we draw is thus that within the one-constant approximation we can transform the stationary shear-flow problem of nematic liquid crystals into the one of a particle of negative mass moving on a smooth sphere. In contrast to what is the usual case in particle mechanics we now are studying a boundary value problem knowing the starting and end points of the particle, and the initial velocity has to be calculated when solving the problem. Even if the concept of a negative mass might be confusing in some respects, we have gained a lot by the particle analogy, because now we are in a position to use all the knowledge of classical mechanics and dynamical systems when dealing with the flow. It should be possible to determine "constants of motion" and to derive stability criteria without explicitly solving the equations.

Finally we ask the question of how much of the particle analogy will survive when we study the case of unequal elastic constants. The answer is that the analogy is still valid in this case, however, we have to map the unit sphere along with its torque pattern onto a surface with a shape which depends on the elastic constant ratios K_1/K_3 and K_2/K_3. This approach is discussed in the pure elastic case by Thurston and Almgren[28] and by Thurston.[29] Another approach which should be equally good is to still work on the unit sphere but instead letting the particle mass get anisotropic in a suitable way.

VIII. DISCUSSION

Although the shearing of a nematic liquid crystal is an experiment which is simple to perform, it turns out to exhibit a host of complexities, which makes it difficult to analyze theoretically. With the assumptions made in Sec. I, the theoretical understanding of the problem is contained in the three coupled, nonlinear differential equations (2.1)–(2.3). It is hard to get any intuitive understanding of the system just by writing them down and furthermore they are solvable only in some special cases. Even in these cases it is a difficult task to determine the

stability of the solutions obtained. This has motivated the geometrical approach to the problem made in this paper, where we have shown how we can get an understanding of the behavior of the system without actually solving its governing equations.

By introducing the unit-sphere description of the director and, furthermore, by plotting the torque field which arises from the shearing of the nematic as well as from the application of an electric or a magnetic field, we have gained a good qualitative understanding of many of the features of the flow. If we by some reason can neglect elasticity we even have solved the problem completely. In this case the director will just move along the field lines until it ends up in one of the singular points of the field or, which happens in some cases, in a closed orbit around the point A on the unit sphere. By introducing elasticity into the problem the situation gets more complex. However, by the particle analogy discussed in Sec. VIII we still can get a decent intuitive understanding of the problem. We also learn where we can find the necessary tools for dealing with the general problem, namely, from the study of two-dimensional dynamical systems. By calculating the eigenvalues of the singular points of the torque field we can determine their stability. Furthermore, these eigenvalues can be used to construct approximate solutions to the flow problem in the vicinity of the stable equilibrium points. The thresholds of the hydrodynamic instabilities which can develop in connection with the unstable equilibrium points can also be calculated.

Even if we have gained a lot of information about the flow without actually solving the governing equations there are, of course, many questions which cannot be answered until we do so. One interesting case is the flow when α_3 is positive and α_2 negative. The torque maps in this case are given by Figs. 4(d)—4(h). There is only one singular point A in these. This is a center and the field lines are closed orbits around this. We want to study the features of the in-plane flow in this case, i.e., the flow where the director lies all the time in the plane of shear (the equator) and is given by $\theta_2=\pi/2$; $\varphi_2=\varphi_2(z)$. The fact that this is a possible solution can immediately be seen by substituting it into Eqs. (2.1)—(2.3). There is one instability which can be regarded as a hydrodynamic analogue to a first-order phase transition connected even with this simple flow.[14] This is denoted the tumbling instability and has been observed experimentally by Cladis and Torza[7,8] and also by Pieranski *et al.*[9,10]

By investigating this instability we are, of course, not guided by the torque maps of Figs. 4(d)—4(h). There is, however, another problem which is connected to this experiment and this is the question whether the in-plane flow is stable against fluctuations which tend to bring the director out of the shearing plane or not. Although in both experiments the tumbling instability was observed, the out-of-plane instability was only observed by Pieranski *et al.* and not by Cladis and Torza. This apparent contradiction might be explained by investigating the torque maps of Figs. 4(d)—4(h). If the director fluctuates out of the plane of shear it will leave the equator and instead land up on a field line close to this. In the case when $\alpha_3/|\alpha_2|$ deviates from unity this field line is ellipselike so in two of the quadrants the director will approach the equator as it follows its new orbit, but in the other quadrants it will draw away from it. Still, however, the new orbit is close to the equator from which the director started. In the case when we neglect elasticity it is thus obvious that the in-plane flow is stable against the out-of-plane instability.

Including elasticity, however, the situation gets more complex and it is easy to understand that at least in some cases we might expect the out-of-plane instability to exist. One case is when $\alpha_3 \ll |\alpha_2|$, performing the experiment with parallel boundary conditions. In this case the director starts in the point B^+ on the unit sphere and the torque field will act destabilizing for the first quarter of the equator. Another case is $\alpha_3 \gg |\alpha_2|$, the boundary conditions being perpendicular. The other two combinations of $\alpha_3/|\alpha_2|$ and boundary conditions will not, however, have a tendency of exhibiting the out of plane instability, at least not until the shearing rates get comparatively large. In the experiments mentioned above, Pieranski *et al.* used parallel boundary conditions while Cladis and Torza, who actually studied a Couette flow, used perpendicular boundary conditions. In both papers $a_3/|a_2|$ was reported to be about 0.01 which corresponds to the torque map of Fig. 4(d). It is then obvious that we expect the out-of-plane instability to be observed by Pieranski *et al.* and not by Cladis and Torza. This conclusion is also confirmed by the stability analysis performed by Högfors and Carlsson.[15]

We conclude by stating that the unit-sphere approach gives a good qualitative understanding of the flow properties of nematic liquid crystals. It can also be used in a simple manner to perform some quantitative calculations. Furthermore, it should be a fruitful starting point for those who want to make detailed calculations of the general flow problem as well as investigations of the stability of the flow.

ACKNOWLEDGMENTS

The author is pleased to acknowledge stimulating discussions with K. Sharp, S. T. Lagerwall, and C. Högfors concerning the problem of nematic flows. This work was supported by the Swedish Natural Science Research Council under Contract No. F-Fu-1449-100.

[1]A. Anzelius, Uppsala Univ. Arsskr. 1 (1931).
[2]C. W. Oseen, Forschr. Chem. Phys. Phys. Chem. **20**, 25 (1929).
[3]F. M. Leslie, Arch. Ration. Mech. Anal. **28**, 265 (1968).
[4]J. L. Ericksen, Arch. Ration. Mech. Anal. **4**, 231 (1960).
[5]O. Parodi, J. Phys. (Paris) **31**, 581 (1970).
[6]T. Carlsson and K. Skarp, Mol. Cryst. Liq. Cryst. **78**, 157 (1981).
[7]P. E. Cladis and S. Torza, Phys. Rev. Lett. **35**, 1283 (1975).
[8]P. E. Cladis and S. Torza, *Colloid and Interface Science* (Academic, New York, 1976), Vol. IV, p. 487.

[9]P. Pieranski, E. Guyon, and S. A. Pikin, J. Phys. (Paris) Colloq. **37**, C13 (1976).
[10]P. Pieranski and E. Guyon, Phys. Rev. Lett. **32**, 924 (1974).
[11]K. Skarp, T. Carlsson, I. Dahl, S. T. Lagerwall, and B. Stebler, *Advances in Liquid Crystal Research and Applications,* edited by L. Bata (Pergamon, Oxford, 1980), p. 573.
[12]T. Carlsson and K. Skarp, Liq. Cryst. (to be published).
[13]P. Manneville, Mol. Cryst. Liq. Cryst. **70**, 223 (1981).
[14]T. Carlsson, Mol. Cryst. Liq. Cryst. **104**, 307 (1984).
[15]C. Högfors and T. Carlsson (unpublished).
[16]T. Carlsson, Mol. Cryst. Liq. Cryst. **89**, 57 (1982).
[17]T. Carlsson, J. Phys. (Paris) **44**, 909 (1983).
[18]P. Pieranski and E. Guyon, Phys. Lett. **49A**, 237 (1974).
[19]P. Pieranski and E. Guyon, Phys. Rev. A **9**, 404 (1974).
[20]R. N. Thurston, J. Appl. Phys. **52**, 3040 (1981).
[21]F. M. Leslie, Adv. Liq. Cryst. **4**, 1 (1979).
[22]T. Carlsson, Institute of Theoretical Physics (Chalmers University of Technology) Report No. 3.85 (1985) (unpublished).
[23]P. Pieranski and E. Guyon, Solid State Commun. **13**, 435 (1973).
[24]P. Manneville and E. Dubois-Violette, J. Phys. (Paris) **37**, 285 (1976).
[25]P. G. de Gennes, *The Physics of Liquid Crystals* (Clarendon, Oxford, 1975), p. 81; and W. H. de Jeu, *Physical Properties of Liquid Crystalline Materials* (Gordon and Breach, New York, 1980), p. 76.
[26]See, e.g., L. Meirovitch, *Elements of Vibrational Analysis* (McGraw-Hill, New York, 1975), Chap. 5.3.
[27]See, e.g., H. Goldstein, *Classical Mechanics* (Addison-Wesley, Reading, Mass., 1980).
[28]R. N. Thurston and F. J. Almgren, J. Phys. (Paris) **42**, 413 (1981).
[29]R. N. Thurston, J. Phys. (Paris) **42**, 419 (1981).